analytical chemistry

pubs.acs.org/ac Article

Development of Improved Double-Nanobody Sandwich ELISAs for Human Soluble Epoxide Hydrolase Detection in Peripheral Blood Mononuclear Cells of Diabetic Patients and the Prefrontal Cortex of Multiple Sclerosis Patients

Dongyang Li, Christophe Morisseau, Cindy B. McReynolds, Thomas Duflot, Jérémy Bellien, Rashed M. Nagra, Ameer Y. Taha, and Bruce D. Hammock*

Cite This: https://dx.doi.org/10.1021/acs.analchem.0c01115 Read Online

ABSTRACT: Nanobodies have been progressively replacing traditional antibodies in various immunological methods. However, the use of nanobodies as capture antibodies is greatly hampered by their poor performance after passive adsorption to polystyrene microplates, and this restricts the full use of double nanobodies in sandwich enzyme-linked immunosorbent assays (ELISAs). Herein, using the human soluble epoxide hydrolase (sEH) as a model analyte, we found that both the immobilization format and the blocking agent have a significant influence on the performance of capture nanobodies immobilized on polystyrene and the subsequent development of double-nanobody sandwich ELISAs. We first conducted epitope mapping for pairing nanobodies and then prepared a horseradish-peroxidase-labeled nanobody using a mild conjugation procedure as a detection antibody throughout the work. The resulting sandwich ELISA using a capture nanobody (A9, 1.25 μg/mL) after passive adsorption and bovine serum albumin (BSA) as a blocking agent generated a moderate sensitivity of 0.0164 OD·mL/ng and a limit of detection (LOD) of 0.74 ng/mL. However, the introduction of streptavidin as a linker to the capture nanobody at the same working concentration demonstrated a dramatic 16-fold increase in sensitivity (0.262 OD·mL/ng) and a 25-fold decrease in the LOD for sEH (0.03 ng/mL). The streptavidin-bridged double-nanobody ELISA was then successfully applied to tests for recovery, cross-reactivity, and real samples. Meanwhile, we accidentally found that blocking with skim milk could severely damage the performance of the capture nanobody by an order of magnitude compared with BSA. This work provides guidelines to retain the high effectiveness of the capture nanobody and thus to further develop the double-nanobody ELISA for various analytes.

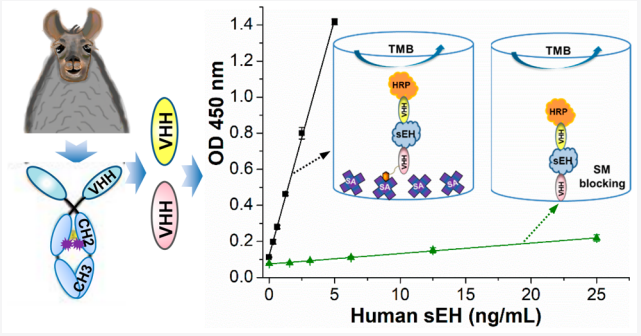

Rapid and sensitive detection technologies are critical for decision-making procedures in many fields, including clinical, food safety, and environmental monitoring fields. The immunoassay is one of the most powerful of all immunochemistry techniques and has been extensively used to detect and quantitate numerous analytes in many applications.[1] Taking *in vitro* diagnostics (IVD) for example, it possessed the highest market share of the IVD market (37%) with sales of $18.6 billion achieved in 2012 and $26.9 billion predicted by 2024.[2,3] Among immunoassays, the enzyme-linked immunosorbent assay (ELISA) has been most used due to its overwhelming overall advantages of high sensitivity, excellent selectivity, simplicity, fast speed, high throughput, low cost, safety, and general applicability.[3,4] The key to an excellent ELISA is the availability of antibodies with high affinity, specificity, and batch-to-batch consistency. However, both academic and industrial communities have been suffering from a reproducibility crisis of antibodies caused by the limited supply and large variance between batches of polyclonal antibodies (pAbs) or the deterioration and loss of hybridomas of monoclonal antibodies (mAbs) in storage.[5] Thus there is a strong demand that "all antibody reagents should be sequenced and then produced from the genetic code obtained".[6]

A nanobody, also termed VHH, is an antibody with a single variable domain derived from heavy-chain-only antibodies in camelids or cartilaginous fish.[7−9] This recombinant antibody is a promising solution to the reproducibility crisis because it can

Received: March 13, 2020
Accepted: April 7, 2020
Published: April 7, 2020

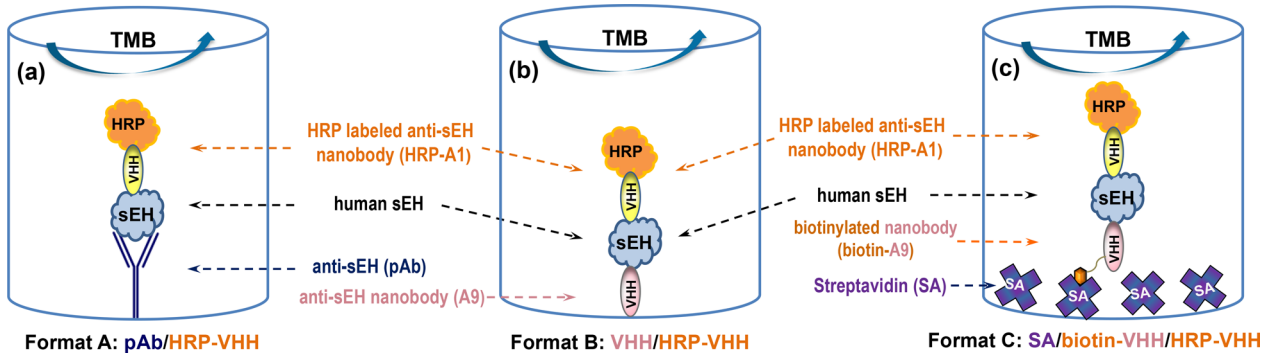

Figure 1. Schematic comparison of three different sandwich ELISA formats for human sEH detection using the same horseradish-peroxidase (HRP)-labeled anti-sEH nanobody conjugate (HRP-A1) as a detection antibody. (a) Format A (pAb/HRP-A1): passively adsorbed polyclonal antibody, (b) format B (A9/HRP-A1): passively adsorbed nanobody, and (c) format C (SA/biotin-A9/HRP-A1): passively adsorbed nanobody biotinylated and bound to streptavidin, as capture antibodies, respectively.

be easily sequenced and resynthesized. Moreover, nanobodies have received increasing interest owing to their small size, monoclonal nature, genetic manipulability, high thermostability, superior solubility, ease of clone storage and expression in diverse expression platforms, and cost effectiveness for both discovery and continuous production.[4,10] This can address not only the issues of the limited supply and the batch-to-batch variation of pAb but also the risk of hybridoma deterioration associated with costly liquid-nitrogen cryogenic storage and the non-mono-specific problem of the classical mAb caused by the frequent expression of additional functional variable regions by hydridomas.[11] It is therefore no wonder that nanobodies are progressively replacing conventional IgG-based antibodies in various immunological techniques, especially in the immunoassay. Our group recently developed many successful immunoassays using nanobodies as detection antibodies for various analytes, including small molecules such as 3-phenoxybenzoic acid,[10] triclocarban,[12] tetrabromobisphenol A,[13] ochratoxin,[14] triazophos,[15] and fipronil[16] as well as large proteins such as soluble epoxide hydrolase[4,17] and cystic fibrosis transmembrane conductance regulator (CFTR) inhibitory factor.[18] However, the use of a nanobody as a capture antibody in classical sandwich ELISAs relying only on fully sequenced nanobodies for both capturing and reporting is greatly hampered by its poor performance after the passive adsorption of the small-size-based nanobody on polystyrene microplates. The fundamental study of the mechanism behind the deterioration of the capture nanobody is lacking, and the physical and functional behaviors of the capture nanobody immobilized on polystyrene remains unexplored. It is important to understand the potential cause of the substantial loss of functionality of capture nanobodies adsorbed on polystyrene microplates and to further improve their performance in ELISAs.

To tackle this problem, we developed two sandwich ELISA formats using nanobodies as capture antibodies and compared them with that using pAb as the capture antibody on polystyrene microplates. Human soluble epoxide hydrolase (sEH) was chosen as the model analyte considering its increasing significance as a biomarker of many diseases[19−25] and the availability of corresponding nanobodies in the laboratory. The basic purpose of this study was to examine the physical and functional behaviors of the capture nanobody immobilized on polystyrene and thus to establish a guideline for developing the double-nanobody ELISA. First, we conducted epitope mapping for pairing nanobodies and then prepared a horseradish-peroxidase (HRP)-labeled nanobody (HRP-A1) as a detection antibody using a mild conjugation method. Second, we compared the performance of a sandwich ELISA for sEH detection using the nanobody (format B, Figure 1b) and the passively adsorbed polyclonal Ab (format A, Figure 1a) as the capture Abs. Third, we evaluated the effect of streptavidin as a bridge for immobilizing the nanobody on polystyrene (format C, Figure 1c) and compared several ways of blocking in this format. Fourth, three ELISAs (formats A, B, and C) were compared in a quantitative way at the same working concentration of the capture antibody. Fifth, bovine serum albumin (BSA) blocking was compared with skim milk (SM) blocking on a polystyrene plate with the passively adsorbed nanobody (format B). Finally, streptavidin-bridged double-nanobody ELISAs were applied to tests for recovery and cross-reactivity and the analysis of real samples with various sEH levels.

EXPERIMENTAL SECTION

Materials. Recombinant human sEH, antihuman sEH rabbit pAb, and eight nanobodies (A1, A9, B1, B3, B4, B6, B7, and B15) were produced, as described in our previous work.[17,26] Horseradish peroxidase (HRP, cat. no. P6782), sodium periodate (311448), sulfo-NHS-LC-biotin (B1022), and streptavidin (S4762) were purchased from Sigma-Aldrich. BSA (BP1600-100) and SM powder (1.15363.0500) were purchased from Fisher Scientific and EMD Millipore, respectively. High-binding polystyrene microplates (Nunc Maxisorp, 442404) were purchased from Thermo Fisher Scientific. A sensitive 3,3′,5,5′-tetramethylbenzidine (TMB) substrate for color development was prepared, as detailed in the Supporting Information (SI). Eight antihuman sEH VHHs were biotinylated against amine groups at a 10:1 molar ratio of sulfo-NHS-LC-biotin to nanobody, as previously described.[4]

Epitope Mapping. Modified from the assay for epitope mapping of mAbs on cells,[27] competition assays based on an indirect immunoassay are herein proposed to determine the epitope specificity of eight antihuman sEH nanobodies that we previously obtained. As shown in Figure S1a, unconjugated nanobodies were incubated with biotinylated nanobodies for competitive binding to human sEH coated on a microplate. The percentage of inhibition (PI) was defined as a ratio between the optical density (OD) of the well with the unconjugated nanobody in excess and the OD obtained for

https://dx.doi.org/10.1021/acs.analchem.0c01115
Anal. Chem. XXXX, XXX, XXX−XXX

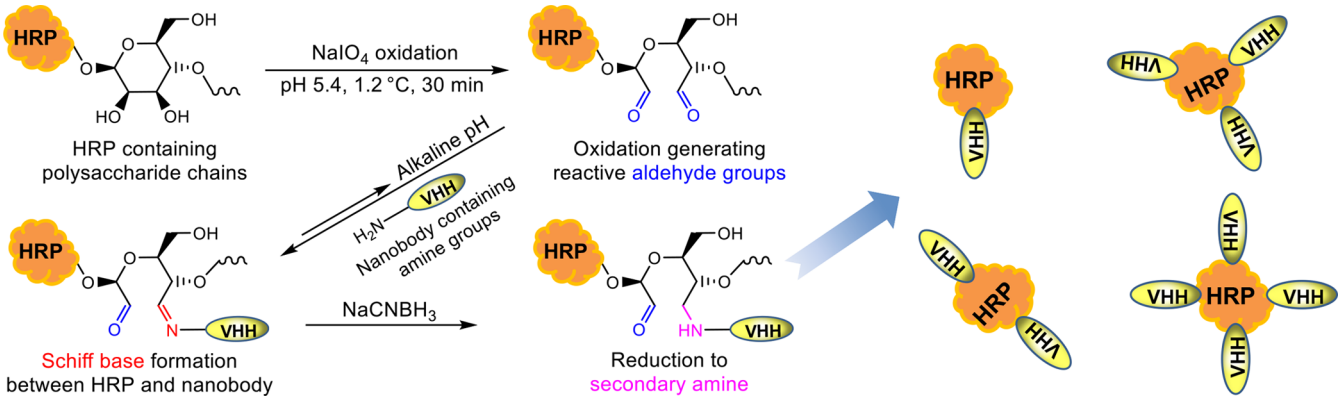

Figure 2. Schematic preparation of the enzyme HRP-labeled nanobody A1 conjugate (HRP-A1) based on a mild periodate oxidation (Malaprade reaction). HRP is a heme-containing glycoprotein that may be oxidized with sodium periodate. The resulting reactive aldehyde residues may be conjugated to a nanobody with a Schiff base formed and further stabilized by sodium cyanoborohydride.

each biotinylated nanobody alone (Figure S1b). Inhibition was regarded as significant when the PI was >50%.[27]

Preparation of HRP-Labeled Nanobody Conjugate (HRP-A1). As illustrated in Figure 2, HRP enzyme was conjugated to the nanobody (A1) through periodate oxidation (Maraprade reaction) but under mild conditions (pH 5.4, 10 mM $NaIO_4$, 30 min, ice bath (1.2 °C)) with a high working concentration of HRP. Fractions without unconjugated monomer after size exclusion chromatography (SEC) were collected and further processed for downstream use as detection antibodies. The detailed preparation and characterization of the HRP-labeled nanobody conjugate are available in the SI.

Comparison of Polyclonal Ab and Nanobody as Capture Antibodies in the ELISA. Antihuman sEH antiserum (1:2000 dilution) or affinity-purified pAb (3 μg/mL) through a protein A column was coated in 0.05 M pH 9.6 carbonate−bicarbonate buffer (CB) overnight at 4 °C on a high-binding Nunc microplate (100 μL/well). Meanwhile, nanobody A9 (20 μg/mL) was coated in CB or phosphate-buffered saline (PBS) on the same plate. After washing, 3% (w/v) SM/PBS (250 μL/well) was added to block the plate for 1 h, and it was subsequently washed. Then, serial concentrations of human sEH standards prepared in PBS containing 0.1 mg/mL BSA were added to the plate (100 μL/well), immediately followed by HRP-A1 in PBS (1:1600, 100 μL/well). After another 1 h of incubation, the immunoreaction was ended with the final washing step. TMB substrate (100 μL/well) was then added to the plate and incubated for 15 min. The color development was then terminated with 1 M sulfuric acid (100 μL/well), and the OD was recorded within 10 min using a microplate reader at 450 nm. All incubations unless otherwise specified were performed with shaking (600 rpm) on a microplate shaker at room temperature, and three washings with PBS containing 0.05% Tween-20 (PBST, 300 μL/well) were conducted in each washing step using a plate washer.

Development of the SBdNb ELISA (Format C) for sEH Detection. Streptavidin (2.5 μg/mL) was coated in CB overnight at 4 °C on a Nunc microplate (100 μL/well). After washing, the plates were blocked with 2% BSA (250 μL/well) for 1 h and then washed. Biotinylated nanobody A9 (BioA9, 1.25 μg/mL, 100 μL) was added to each well. After 1 h of incubation and then washing, serial human sEH standards (100 μL/well) were added to the plate and then immediately followed by the addition of varying concentrations of detection antibody HRP-A1 (1:1600−1:12 800, 100 μL/well) in PBS or 10% SM/PBS. After another 1 h of incubation and then the final washing, the color was developed for 15 min with TMB and stopped with sulfuric acid. The OD was recorded at 450 nm. Prior optimization of streptavidin and BioA9 is detailed in Figure S4.

Comparison of Three Formats at the Same Working Concentration of Capture Antibodies. The SBdNb ELISA and the other two formats (A and B) were simultaneously compared with two Nunc microplates used. Streptavidin (2.5 μg/mL) was coated in CB overnight at 4 °C on plate I, and the SBdNb ELISA was run on this plate, as previously described. For plate II, pAb (1.25 μg/mL in CB), A9 (1.25 μg/mL in PBS), and A9 (20 μg/mL in PBS) were coated overnight at 4 °C (100 μL/well) on columns 1−3, 4−6, and 7−12, respectively. After washing, plate II was blocked with 2% BSA (columns 1−9) or 3% SM (columns 10−12) at 250 μL per well, and this blocking was simultaneously conducted with the addition of BioA9 (1.25 μg/mL) on plate I. After 1 h of incubation, both plates were washed, and then human sEH standards plus HRP-A1 (1:6400) were added in one step. After another 1 h of incubation, both plates were simultaneously washed, incubated with TMB, and finished with an OD reading, as previously described.

BSA versus SM in Blocking of Microplate with Passively Adsorbed Nanobody. Varying concentrations of nanobody A9 (0.625−20 μg/mL) were directly coated in PBS overnight at 4 °C on a Nunc microplate. After washing, both plates were simultaneously blocked with 2% BSA or 3% SM (half plate for each blocking agent, 250 μL/well) for 1 h. Subsequently, the same downstream steps as those of the aforementioned format A were performed.

Cross-Reactivity. The cross-reactivity of the SBdNb ELISA was evaluated by its sensitivity for an interferent relative to that for the target analyte. A group of epoxide hydrolases was tested.

Matrix Effects. The SBdNb ELISA was applied to brain tissue samples from sEH knockout (KO) mice. A simple dilution protocol was followed to evaluate the matrix effect. In brief, the brain tissue samples were diluted with standard diluent (PBS containing 0.1 mg/mL BSA) to 1:150, 1:450, and 1:1350. Subsequently, spiked samples were obtained by spiking a series of human sEH solutions into samples of various dilutions and analyzed with the SBdNb ELISA.

https://dx.doi.org/10.1021/acs.analchem.0c01115
Anal. Chem. XXXX, XXX, XXX−XXX

Real Sample Analysis. S9 fractions from pooled (4−50 individuals) human tissues of six kinds purchased from Xenotech (Lenexa, KS), peripheral blood mononuclear cell (PBMC) samples from patients without or with type 2 diabetes, and post-mortem brain samples from patients without or with multiple sclerosis were serially diluted with standard diluent and analyzed with the SBdNb ELISA. Dilutions resulting in OD readings in the linear range of the calibration curve were adopted to calculate the human sEH level in the samples.

RESULTS AND DISCUSSION

Epitope Mapping and the Preparation of HRP-Labeled Nanobody Conjugate (HRP-A1). The classical sandwich ELISA captures the analytes using the capture antibody immobilized on the microplate and subsequently detects them with an enzyme-labeled detection antibody. Theoretically, double-nanobody-based sandwich ELISAs in such a classical and simple format (as shown in Figure 1b) can be developed and could fully replace the classical sandwich format using double Abs of pAb or mAb. As is true with antibodies, it is ideal to use a pair of nanobodies recognizing different epitopes in the sandwich ELISA. This procedure utilizes the formation of a sandwich immunocomplex, resulting in increased selectivity. As illustrated in Figure S1, the eight nanobodies were divided into six groups of mutually noncompetitive antibodies as follows: group I (A1, B4, B7), group II (A9), group III (B1), group IV (B3), group V (B6), and group VI (B15). This also means that the six groups of nanobodies recognize six different epitopes of human sEH. Considering their high yield of expression and good affinity, A1 from group I and A9 from group II were chosen as the pair in this work for the double-nanobody ELISA development. A1 is used to conjugate the enzyme label because it has been well validated as a detection antibody after biotinylation elsewhere.[4]

As illustrated in Figure 2, HRP enzyme was conjugated to the nanobody (A1) through periodate oxidation (Maraprade reaction) but under mild conditions (pH 5.4, 10 mM $NaIO_4$, 30 min, ice bath (1.2 °C)). This revised working condition is much milder than that of periodate oxidation in the classical literature for preparing HRP-labeled IgG Ab.[28] It can not only better retain the enzyme activity of the oxidized HRP but also avoids the formation of HRP polymer caused by overoxidation. In addition, unlike IgG, the unique small size of the nanobody allowed a clearer separation of the HRP, antibody, and conjugates in the resulting mixture through SEC, and thereby a harvest of the conjugates with unconjugated monomers eliminated. This is very meaningful because the free antibody can suppress the specific signal of the conjugates, and the unconjugated enzyme can cause increased nonspecific background. Together, they may greatly reduce the signal-to-noise ratio. The synthesis, purification, and characterization of HRP-labeled nanobody conjugates are detailed in the SI. Eventually, the resultant purified HRP-A1 conjugates possess an average of 3 nanobodies conjugated per HRP according to the densitometry on SDS-PAGE (Figure S2c) or 1.8 nanobodies per HRP calculated from their adsorption at 280 and 403 nm. As shown in Figure S3, the optimal working concentration of the HRP-A1 conjugate obtained is 1:1600 for the sandwich ELISA (format A) in terms of sufficient signal and low background, using antiserum at 1:2000 (the same coating as that in ref 4) as the capture antibody and 3% SM for plate blocking. The sensitivity obtained under this condition is around one-fourth of that in the previously published ultrasensitive PolyHRP ELISA,[4] indicating the high potency of the HRP-labeled nanobody.

Comparison of ELISA Formats Using Polyclonal Ab and Nanobody as Capture Antibodies. To fully replace traditional antibodies in immunoassay, it is crucial that nanobodies can demonstrate superior or at least comparable performance to classical pAbs of IgG type as both detection and capture antibodies. The aforementioned studies indicated the satisfactory performance of nanobodies as detection antibodies with the extra advantages of excellent solubility and superior penetration. However, the performance comparison between IgG and the nanobody as a capture antibody in a quantitative way is rarely seen. Thus we evaluated the capture performance of the pAb and nanobody reagents by comparing ELISA formats A and B, as shown in Figure 1. However, for comparison, it is important to have a proper parameter as an index of the performance. For the study of pAb and mAb, Butler et al. defined and introduced the parameter of antigen capture capacity (AgCC) as a reflection of the antibody activity or affinity. AgCC equals $[Ag]_b/[Ag]_t$. It is expressed as a percent, where $[Ag]_b$ is the amount of Ag bound in the linear binding region (the region of capture Ab in excess) at a high dilution of antigen, and $[Ag]_t$ is the total amount of antigen added. They used iodinated antigen for tracing and quantification. This parameter tends to be constant in the linear binding region.[29] In our work, we adopted sensitivity (slope) in the linear range as a direct measure of the immunoactivity of the nanobody immobilized on polystyrene. This parameter eliminates the obscurity of AgCC, making quantitative comparisons simple and straightforward. Figure 3 shows the signal responses of two ELISAs (formats A and B) run under the same conditions for human sEH detection. For format B, 20 μg/mL nanobody coated in 10 mM PBS (pH 7.4) buffer generated 38% higher assay sensitivity (0.0116 OD·mL/

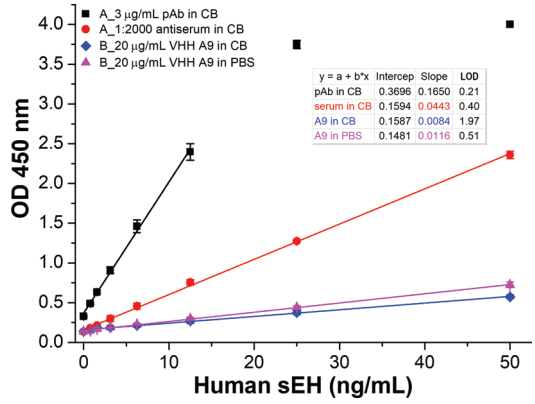

Figure 3. Signal responses of four ELISAs in two formats (A and B) run on the same plate using HRP-VHH A1 (1:1600 dilution) as the detection antibody. For format A, anti-sEH affinity-purified polyclonal antibody (pAb, 3 μg/mL) or antiserum (1:2000 dilution) was used as the capture antibody through passive adsorption on a high-binding polystyrene microplate. For format B, nanobody A9 (20 μg/mL) coated in CB or PBS buffer was used as the capture antibody after passive adsorption. The four ELISAs were performed on the same plate using 3% skim milk (SM) for blocking after the coating step. The same reagents involved for different formats are used from the same prepared batch. All same or similar steps were performed at the same time under the same conditions. Error bars indicate standard deviations (n = 3). All coefficients of determination R^2 > 0.99.

https://dx.doi.org/10.1021/acs.analchem.0c01115
Anal. Chem. XXXX, XXX, XXX−XXX

ng) than that coated in CB (0.0084 OD·mL/ng), indicating PBS to be a superior coating buffer to CB for nanobody A9. This is, however, much lower than that of format A. Format A using affinity-purified pAb (3 μg/mL, purified through a protein A column with a yield of 6 mg pAb per milliliter of antiserum) and antiserum (1:2000 dilution) as capture antibodies demonstrated sensitivities of 0.1650 and 0.0443 OD·mL/ng, respectively. It is astonishing that 20 μg/mL nanobody (17 kDa, monovalent) gave only 7% of the assay sensitivity of 3 μg/mL pAb (150 kDa, divalent) as the capture antibody, as the former contains 29.4 times more (or 294 times, supposing that antigen-specific pAb accounts for only 10% IgG[1]) antigen-binding sites compared with the latter. It was unclear in that microenvironment what exactly caused the dramatic deterioration of the passively adsorbed capture nanobody on the high-binding polystyrene microplate.

Development of the Streptavidin-Bridged Double-Nanobody ELISA. Butler et al. found that only <3% of the binding sites of mAb and about 5−10% of those of pAb were capable of capturing antigens after passive adsorption on polystyrene. They also surprisingly found that >70% capture capability could be preserved when the antibodies were immobilized via a streptavidin bridge, that is, the protein−(strept)avidin−biotin capture (PABC) system.[30,31] Thus we tried a similar strategy to evaluate the possibility of improving the capture performance of a nanobody on polystyrene. However, a direct coating of streptavidin rather than PABC was used. As shown in Figure 4a, the streptavidin-bridged double-nanobody ELISA (SBdNb ELISA, format C) demonstrated a dramatic OD signal enhancement with sensitivity of 0.4447 OD·mL/ng achieved at the working concentrations of 2.5 μg/mL, 1.25 μg/mL, and 1:1600 dilution for streptavidin, biotin-A9, and HRP-A1, respectively. This improved sensitivity is 38 times that of format B (Figure 3) but with just 1/16 the amount of the capture nanobody used. This huge increase in sensitivity demonstrated the excellent capability of the streptavidin bridge to retain the substantial functional activity of the immobilized capture nanobody. We thought there might be two roles of the streptavidin in the preservation of nanobody functionality. One is that the streptavidin works as an insulating gasket that prevents the nanobody from contacting polystyrene and the consequent denaturation. The other is that it acts as a giant booster seat or stepping stone anchored in the deep polystyrene groove for better exposure of the capture nanobody to antigen, as the polystyrene surface is not atomically flat, and cavities of up to 5 μm and from 10 to 40 nm in depth were observed in Nunc Maxisorp plate with an atomic force microscope,[32] yet it is unclear if these or other mechanisms account for the dramatic role of streptavidin in this protection phenomenon. In addition, it is meaningful to optimize the working concentrations of the assay so as to conserve reagents while maintaining the performance. As shown in Figure S4, 2.5 μg/mL was chosen for streptavidin coated in CB and 1.25 μg/mL was chosen for biotin-A9 in PBS after optimization by varying the working concentrations of streptavidin (10, 5, 2.5, 1.25, and 0.625 μg/mL) and biotin-A9 (5, 2.5, 1.25, and 0.625 μg/mL). For the streptavidin-coated solid phase, SM should not be used as the blocking agent because it contains endogenous biotins that may occupy the biotin-binding sites of immobilized streptavidin and consequently prevent the biotinylated antibody from binding. This interference was first observed in immunoblotting using streptavidin for coating and SM for blocking.[33] It was also

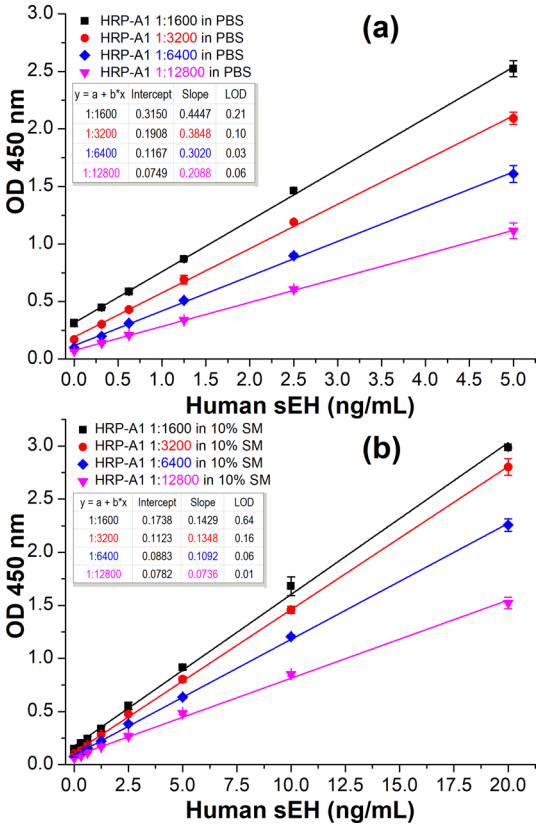

Figure 4. Calibration curves of SBdNb ELISAs (format C) with varying concentrations of the detection antibody (HRP-A1, 1:1600−1:12 800 dilution) in (a) PBS or (b) 10% SM/PBS. Other conditions: streptavidin, 2.5 μg/mL coated in CB overnight at 4 °C; blocking buffer, 2% BSA/PBS 1 h; biotin-A9, 1.25 μg/mL 1 h; HRP-A1, 1 h; TMB 15 min. All same or similar steps were performed under the same conditions (e.g., incubation time, reagents). Error bars indicate standard deviations (n = 3). All coefficient of determination R^2 > 0.99.

confirmed in the SBdNb ELISA that the SM blocking gave a very weak signal response, whereas the BSA blocking showed the opposite. (See Figure S4a,f.) Therefore, the avoidance of SM blocking is crucial to the SBdNb ELISA. As an alternative to SM, BSA blocking allowed high sensitivity but also high background (OD > 0.3) when HRP-A1 at 1:1600 was used. This increased background is attributed to the weaker blocking efficacy of BSA compared with SM.[34] The latter contains small caseins, enabling deeper penetration and thus more efficient blocking of the plate. Besides sensitivity, the limit of detection (LOD) is another important index related to detectability. It is the lowest quantity of an analyte that can be distinguished from the absence of that analyte (a blank value) with a specified confidence level (generally 99%)[35] and hence is a statistical parameter. LOD = $3S_B/k$ refers to the calculated analyte concentration corresponding to signal response of the blank plus three times its standard deviation and is used with units of ng/mL throughout this work, where k is the slope or sensitivity obtained in the linear regression analysis and S_B is the standard deviation of the blank. The LOD is not only determined by the sensitivity but also by the standard deviation of the blank. Therefore, higher sensitivity may mean increased odds of lower LOD but cannot guarantee it, as is shown in Figures 3−5. Although the background signal above does not determine the sensitivity and detectability of an assay, a clean or weak background is always preferred by the

https://dx.doi.org/10.1021/acs.analchem.0c01115
Anal. Chem. XXXX, XXX, XXX−XXX

end users. To decrease the background, normally caused by nonspecific adsorption of the tracer, decreasing the working concentration of HRP-A1 or adding blocking proteins in the tracer was performed. As illustrated in Figure 4a, decreasing HRP-A1 led to a decrease in both the background and the sensitivity. For HRP-A1 diluted in 1:6400 and 1:12 800, an acceptable clean background of OD around 0.1 was achieved with sufficient sensitivity comparable to the PolyHRP ELISA previously published;[4] the linearity can be extended to 10 ng/mL (data not shown), and the LOD is 0.03 and 0.06 ng/mL, respectively. On the contrary, using 10% SM in PBS as the diluent of HRP-A1 also significantly reduced the background (Figure 4b) because SM is a potent blocker that outcompetes the HRP-A1 for nonspecific binding sites. BSA was not adopted because it showed a modest effect as a simultaneous blocking agent in other ELISAs developed in our lab (data not shown). Similar phenomena revealing the efficacy of SM and the inefficacy of BSA for simultaneous blocking were previously observed in immunohistology as well.[36] Despite decreased background due to SM, the sensitivities (Figure 4b) also dropped remarkably with only around 1/3 remaining compared with those of corresponding dilutions of HRP-A1 in PBS illustrated in Figure 4a. The decrease in sensitivity is likely due to the SM containing endogenous biotin,[33] which probably displaced 2/3 of the previously bound biotinylated capture nanobody (biotin-A9) from the streptavidin-coated plate. It is worth noting that the high affinity of streptavidin for free biotin (K_a = 10^{15} M^{-1}) actually does not hold for biotinylated macromolecules, probably because of the steric hindrance caused by the linked proteins. Vincent and Samuel found that the affinity of biotinylated macromolecules to streptavidin decreased by orders of magnitude compared with that of free biotin to streptavidin.[37] Thus the prevalent idea that the binding between streptavidin and biotinylated biomolecules is almost irreversible should be treated with caution. This also means that the risk of competition or displacement from the second biotinylated probe (especially if it is in excess) with the first one can happen when free streptavidin is used to connect two biotinylated probes, for example, the aforementioned PABC system. Therefore, it is important to use direct coating of streptavidin and to avoid SM in the SBdNb ELISA. Considering the balance among the background, sensitivity, and cost efficiency, the SBdNb ELISA with HRP-A1 in 1:6400 dilution, illustrated in Figure 4a, was chosen as the optimal condition and was used for downstream selectivity, recovery, and real sample tests.

Comparison of the SBdNb ELISA and Two Other ELISA Formats. As previously described, the SBdNb ELISA demonstrated excellent performance thanks to the streptavidin bridge. To precisely evaluate the influence of the antibody type and the streptavidin bridge on the functionality of capture antibodies, it is meaningful to compare the SBdNb ELISA (format C) with other formats at the same working concentration of the capture antibody. Figure 5a shows the signal responses of formats A and C using the same concentration (1.25 μg/mL) of pAb and biotinylated nanobody (BioA9) as capture antibodies, respectively. Format C generated a sensitivity (0.2619 OD·mL/ng) that is 3.1 times that of format A (0.0834 OD·mL/ng), with the advantage of the nanobody containing more antigen binding sites probably revealed at the same mass compared with pAb. Moreover, format C gave a lower background than format A. This is likely due to the single domain nature of the nanobody devoid of the

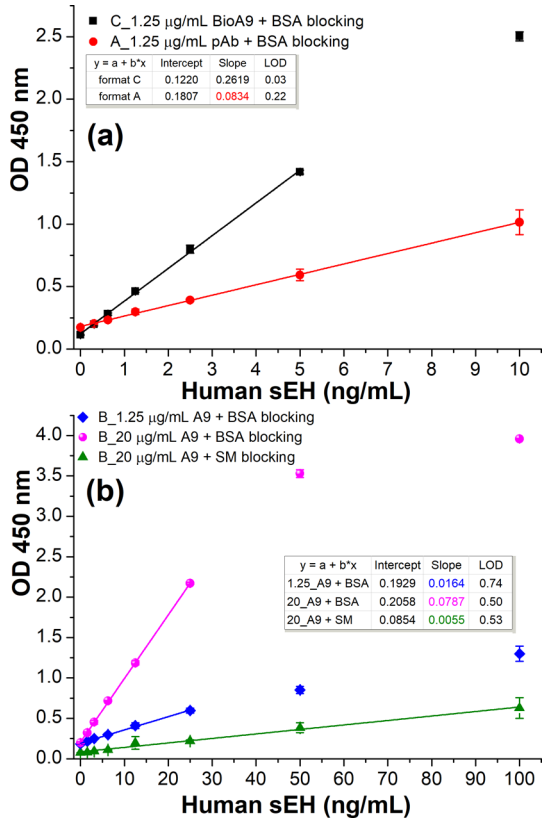

Figure 5. Comparison of three ELISA formats using HRP-A1 (1:6400 dilution in PBS) as the detection antibody. (a) Format C (SBdNb ELISA, ■): 2.5 μg/mL streptavidin, 2% BSA/PBS blocking, 1.25 μg/mL biotin-A9; format A (●): 1.25 μg/mL anti-sEH pAb, 2% BSA/PBS blocking. (b) Format B with varying nanobody A9 coated in PBS and different blocking agents: ◆, 1.25 μg/mL A9 plus 2% BSA/PBS blocking; ●, 20 μg/mL A9 plus 2% BSA/PBS blocking ;▲, 20 μg/mL A9 plus 3% SM/PBS blocking. All same or similar steps were performed under the same conditions. Error bars indicate standard deviations (n = 3). All R^2 > 0.99, except for the ▲ of panel b (R^2 = 0.9878).

Fc portion. In addition, the SBdNb ELISA demonstrated the magic of the streptavidin bridge when compared with format B with 1.25 μg/mL nanobody A9 directly coated. Its sensitivity is 16 times that of format B (Figure 5b, ◆, 0.0164 OD·mL/ng). In other words, <6% nanobody adsorbed passively on polystyrene is still effective for antigen binding. Thus we can conclude that the procedure used to immobilize the nanobody is crucial to the functionality of the capture nanobody. Moreover, it is worth noting that format B (Figure 5b, diamond) has 141% sensitivity compared with the ELISA (format B) described in Figure 3, where PBS was used as the coating buffer, although the working concentrations of the capture nanobody and HRP-A1 in the latter are 16 times and 4 times higher than those of the former, respectively. This unexpected increased sensitivity is likely due to the switch of the blocking agent from 3% SM/PBS to 2% BSA/PBS. It seems that SM not only reduced the nonspecific background but also shielded a substantial specific signal in format B. This was further confirmed by the parallel ELISAs of format B using 20 μg/mL A9 for direct coating (passive adsorption) followed by 2% BSA or 3% SM for blocking. (See Figure 5b.) The SM-blocking-based direct double-nanobody ELISA demonstrated only 7% sensitivity of the BSA blocking-based assay. That

https://dx.doi.org/10.1021/acs.analchem.0c01115
Anal. Chem. XXXX, XXX, XXX−XXX

means that at least 93% of the adsorbed capture nanobody lost its functionality or effectiveness because of SM blocking. There is the question of whether SM disabled more capture nanobody (e.g., through changing its conformation or masking paratopes) due to its nature alone or if it stripped more adsorbed nanobody off polystyrene than did BSA during blocking. The answer to this remains unclear, and further investigation is needed.

Systematic Comparison of BSA Blocking and SM Blocking in Format B. The radical difference in blocking the plate with BSA versus SM was previously demonstrated with a high coating concentration of nanobody (20 μg/mL). To further evaluate this difference, varying coating concentrations (0.625−20 μg/mL) of capture nanobody A9 were passively adsorbed and later blocked with BSA or SM in parallel for each on the same high-binding polystyrene microplate (Nunc Maxisorp). As illustrated in Figure 6, the sensitivity increased

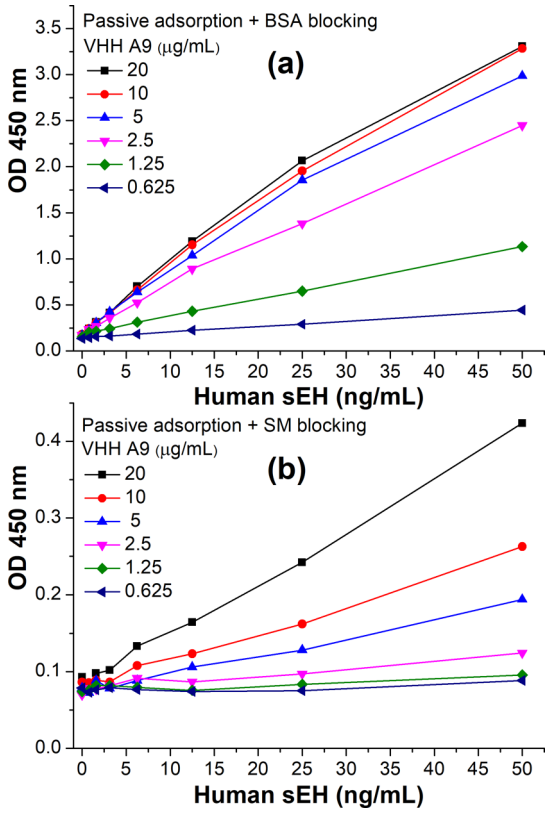

Figure 6. Comparison of ELISA format B using different blocking reagents with varying working concentrations of capture nanobody A9 (0.625−20 μg/mL). The direct coating of A9 (format A) through passive adsorption was followed by (a) 2% BSA blocking or (b) 3% SM blocking. HRP-A1 (1:6400 dilution in PBS) was used as the detection antibody.

with increasing coating concentrations of the capture nanobody under both blocking conditions. For BSA blocking, the saturation of sensitivity occurred at 5 μg/mL of capture A9 (Figure 6a), whereas for SM blocking, shown in Figure 6b, a huge drop in the sensitivity by an order of magnitude was observed in various coating concentrations of nanobodies compared with the BSA-blocking-based situation. Thus we can conclude that the passively adsorbed capture nanobody could retain good functionality with BSA blocking, and SM blocking should be avoided due to its severe damage to the efficacy of the capture nanobody. On the contrary, format B demonstrated one-fourth the sensitivity of the optimized SBdNb ELISA when a 5 μg/mL saturation of A9 was used as the optimal coating concentration, although the former used four times more nanobody. This sensitivity is actually sufficient for detecting many real samples where the sEH abundance is not too low. Compared with the SBdNb ELISA, format B based on passive adsorption of the capture nanobody saved the steps of the streptavidin bridge and the biotinylation of the nanobody, however, at the cost of a dramatic loss of antibody efficiency, that is, with no more than 1/16 functionality per nanobody amount remaining.

Validation of the SBdNb ELISA. On the basis of the aforementioned comparison of three ELISA formats, the SBdNb ELISA (format C) turned out to be the superior double-nanobody ELISA in terms of sensitivity as well as the reagent's cost-effectiveness and thus was used for further validation. As detailed in Table S1, the SBdNb ELISA demonstrated excellent selectivity for the target, allowing the specific detection of only the bioactive sEH, with negligible interference from epoxide hydrolases in the same enzyme family, such as human mEH and human EH3. Moreover, the matrix effects were evaluated through spike-and-recovery tests against spiked samples at varying dilutions. As detailed in Table S2, the background decreased, and the net signal increased with increasing dilutions of the sample matrix of sEH-free mouse brain tissue. The recovery was 75−98, 78−90, and 78−97% for the spiked samples prepared at 1:150, 1:450, and 1:1350 dilution of the sample matrix, respectively. The corresponding overall recovery was 75, 84, and 91%, respectively. These data support the acceptance of the SBdNb ELISA for sEH detection in biological samples. Furthermore, a successful analytical approach must satisfy the need for the detection of real samples with high accuracy.[38] The SBdNb ELISA was used to analyze the sEH in the S9 fractions of pooled (4−50 persons) human tissue samples described in the SI. The resultant data were compared with those obtained through the enzyme-activity-based radiometric assay, Western blot, the conventional ELISA, the NbS7/NbS43 ELISA, and the PolyHRP ELISA (Table S3). We can find that the data by the SBdNb ELISA are comparable to those by the other five methods. Moreover, the SBdNb ELISA showed good correlation to the radioactive assay in these tissue samples, with a correlation coefficient of $r > 0.99$, suggesting that the sEH protein level through the SBdNb ELISA is a good indication of its enzyme activity. Also, as specified in Tables S4 and S5, the SBdNb ELISA successfully measured PBMC samples from patients without or with type 2 diabetes and brain samples from patients without or with multiple sclerosis, respectively. In general, PBMCs have a very low abundance of sEH and thus require assays of high sensitivity. The results obtained through the SBdNb ELISA well disclosed the association between the sEH overexpression and the pathogenesis of type 2 diabetes as well as the lack of a correlation between sEH and the progression of multiple sclerosis. This further indicates the significance of the SBdNb ELISA as an important diagnostic tool for human health.

Further Overall Discussion. Interestingly, Zhu et al. reported a streptavidin−biotin-based directional double-nanobody sandwich ELISA for the detection of influenza H5N1. The capture nanobody was biotinylated in vivo at the opposite terminal of the antigen-binding site and later bound to a commercial streptavidin-coated microplate for a directional

https://dx.doi.org/10.1021/acs.analchem.0c01115
Anal. Chem. XXXX, XXX, XXX−XXX

immobilization with the paratope facing outward. The resultant directional ELISA was claimed to show more sensitivity than the undirectional conventional ELISA involving passive adsorption of the capture nanobody and BSA blocking.[39] However, the sensitivities of both ELISAs are moderate and seem to be comparable. A confirmative comparison is difficult to make in view of the limited quality of the linear fitting. Also, Rossotti et al. developed a sensitive double-nanobody-based indirect sandwich ELISA for sEH detection using avidin as a bridge on polystyrene plates. This format was adopted as the adaptation to a screening platform they proposed, where the output clones were first biotinylated in vivo in 96-well culture plates and then bound to avidin-coated microplates for immobilization. Clones with high affinity were ranked according to their reactivity with the HRP-labeled antigen.[40] Actually, their avidin-bridged indirect sandwich ELISA is similar to our SBdNb ELISA. We therefore inferred that the high sensitivity of the assay is not only due to nanobodies of high affinity obtained alone but also due to the bioactivity enhancement of the avidin bridge. Despite the emergence of some early research on developing the double-nanobody-based ELISA, the field has mainly focused on the analytical aspects. The exploration of other factors contributing to the performance of capture nanobodies has been rare in the literature.

CONCLUSIONS

We developed an improved double-nanobody sandwich ELISA for human sEH detection. Epitope mapping was successfully performed to pair nanobodies for the sandwich immunoassay, and HRP-labeled nanobody conjugate as a detection antibody was favorably prepared through an improved periodate oxidation in a much milder but efficient conjugation manner. Compared with the double-nanobody ELISA with the capture nanobody passively adsorbed on the polystyrene microplate, the streptavidin-bridged double-nanobody ELISA demonstrated a 16 times higher sensitivity and a 25 times lower LOD compared with the former, with the sensitivity improved from 0.0164 to 0.2619 OD·mL/ng and the LOD improved from 0.74 to 0.03 ng/mL for human sEH detection. The enhanced ELISA was then successfully applied to tests for the recovery and cross-reactivity and the analysis of real samples. Meanwhile, blocking with SM was unexpectedly found to severely damage the performance of the passively adsorbed capture nanobody by an order of magnitude compared with blocking with BSA. Thus understanding the physical and functional behaviors of the capture nanobodies immobilized on polystyrene related to both the immobilization format and the blocking agent provides a general guideline for developing double-nanobody ELISAs for various targets.

ASSOCIATED CONTENT

Supporting Information

The Supporting Information is available free of charge at https://pubs.acs.org/doi/10.1021/acs.analchem.0c01115.

Supplementary experimental section, epitope mapping of nanobodies, characterization of the HRP-labeled nanobody, optimization of HRP-A1 working concentration, optimization of SA and BioA9, selectivity of the SBdNb ELISA, recovery test, S9 fraction of human tissues analysis, analysis of PBMCs from diabetic patients, and analysis of brain samples from MS patients (PDF)

AUTHOR INFORMATION

Corresponding Author

Bruce D. Hammock − *Department of Entomology and Nematology and UCD Comprehensive Cancer Center, University of California, Davis, California 95616, United States;* orcid.org/0000-0003-1408-8317; Email: bdhammock@ucdavis.edu

Authors

Dongyang Li − *Department of Entomology and Nematology and UCD Comprehensive Cancer Center, University of California, Davis, California 95616, United States;* orcid.org/0000-0002-5603-3608

Christophe Morisseau − *Department of Entomology and Nematology and UCD Comprehensive Cancer Center, University of California, Davis, California 95616, United States*

Cindy B. McReynolds − *Department of Entomology and Nematology and UCD Comprehensive Cancer Center, University of California, Davis, California 95616, United States*

Thomas Duflot − *Department of Clinical Pharmacology, Rouen University Hospital & Institut National de la Santé et de la Recherche Médicale (INSERM) U1096, Normandie University, UNIROUEN, Rouen 76031, France;* orcid.org/0000-0002-8730-284X

Jérémy Bellien − *Department of Clinical Pharmacology, Rouen University Hospital & Institut National de la Santé et de la Recherche Médicale (INSERM) U1096, Normandie University, UNIROUEN, Rouen 76031, France*

Rashed M. Nagra − *Neurology Research, West Los Angeles VA Medical Center, Los Angeles, California 90073, United States*

Ameer Y. Taha − *Department of Food Science and Technology, University of California, Davis, California 95616, United States;* orcid.org/0000-0003-4611-7450

Complete contact information is available at: https://pubs.acs.org/10.1021/acs.analchem.0c01115

Author Contributions

D.L. and B.D.H. designed the research; D.L. and C.M. performed the experiment; T.D. and J.B. provided PBMCs samples; R.M.N., A.Y.T., and B.D.H. designed the clinical applications involving human post-mortem samples; and D.L., C.M., C.B.M., and B.D.H. analyzed data and wrote the paper.

Notes

The authors declare no competing financial interest.

ACKNOWLEDGMENTS

This work was financially supported by the National Institutes of Health (NIEHS Superfund P42ES04699 and RIVER Award R35 ES030443-01). D.L. received partial support from the National Natural Science Foundation of China (81402722) and The International Postdoctoral Exchange Fellowship (06/2014-06/2015) by The Office of China Postdoctoral Council. C.B.M. received support from the NIH Training Program in Chemical Biology (T32 GM113770). A.Y.T. and R.M.N. received support from the National Multiple Sclerosis Society (PP-1606-24495 and RG 829-P-40).

REFERENCES

(1) Harlow, E.; Lane, D. *Antibodies: A Laboratory Manual*; Cold Spring Harbor Laboratory: New York, 1988; p 291.
(2) Huckle, D. In *The Immunoassay Handbook*, 4th ed., Wild, D., Ed.; Elsevier: Oxford, U.K., 2013; pp 517−531.
(3) VynZ Research. Global Immunoassay Market is Set to Reach USD 26.9 Billion by 2024, Growing at a CAGR of 5.6% During the Forecast Period, 2019. https://www.globenewswire.com/news-release/2019/07/09/1879881/0/en/Global-Immunoassay-Market-is-Set-to-Reach-USD-26-9-Billion-by-2024-Growing-at-a-CAGR-of-5-6-During-the-Forecast-Period-VynZ-Research.html (accessed March 12, 2020).
(4) Li, D.; Cui, Y.; Morisseau, C.; Gee, S. J.; Bever, C. S.; Liu, X.; Wu, J.; Hammock, B. D.; Ying, Y. *Anal. Chem.* **2017**, *89*, 6248−6256.
(5) Baker, M. Reproducibility Crisis: Blame it on the Antibodies. *Nature* [Online] **2015**. http://www.nature.com/news/reproducibility-crisis-blame-it-on-the-antibodies-1.17586 (accessed March 12, 2020).
(6) Arnaud, C. H. Call For Antibody Standardization. *C&EN News* [Online] **2015**. http://cen.acs.org/articles/93/web/2015/02/Call-Antibody-Standardization.html (accessed March 12, 2020).
(7) Greenberg, A. S.; Avila, D.; Hughes, M.; Hughes, A.; McKinney, E. C.; Flajnik, M. F. *Nature* **1995**, *374*, 168−173.
(8) Hamers-Casterman, C.; Atarhouch, T.; Muyldermans, S.; Robinson, G.; Hammers, C.; Songa, E. B.; Bendahman, N.; Hammers, R. *Nature* **1993**, *363*, 446−448.
(9) Steeland, S.; Vandenbroucke, R. E.; Libert, C. *Drug Discovery Today* **2016**, *21*, 1076−1113.
(10) Kim, H.-J.; McCoy, M. R.; Majkova, Z.; Dechant, J. E.; Gee, S. J.; Tabares-da Rosa, S.; González-Sapienza, G. G.; Hammock, B. D. *Anal. Chem.* **2012**, *84*, 1165−1171.
(11) Bradbury, A. R.; Trinklein, N. D.; Thie, H.; Wilkinson, I. C.; Tandon, A. K.; Anderson, S.; Bladen, C. L.; Jones, B.; Aldred, S. F.; Bestagno, M. *MAbs* **2018**, *10*, 539−546.
(12) Tabares-da Rosa, S.; Rossotti, M.; Carleiza, C.; Carrión, F.; Pritsch, O.; Ahn, K. C.; Last, J. A.; Hammock, B. D.; González-Sapienza, G. *Anal. Chem.* **2011**, *83*, 7213−7220.
(13) Wang, J.; Bever, C. R.; Majkova, Z.; Dechant, J. E.; Yang, J.; Gee, S. J.; Xu, T.; Hammock, B. D. *Anal. Chem.* **2014**, *86*, 8296−8302.
(14) Liu, X.; Xu, Y.; Wan, D. B.; Xiong, Y. H.; He, Z. Y.; Wang, X. X.; Gee, S. J.; Ryu, D.; Hammock, B. D. *Anal. Chem.* **2015**, *87*, 1387−1394.
(15) Wang, K.; Liu, Z.; Ding, G.; Li, J.; Vasylieva, N.; Li, Q. X.; Li, D.; Gee, S. J.; Hammock, B. D.; Xu, T. *Anal. Bioanal. Chem.* **2019**, *411*, 1287−1295.
(16) Wang, K.; Vasylieva, N.; Wan, D.; Eads, D. A.; Yang, J.; Tretten, T.; Barnych, B.; Li, J.; Li, Q. X.; Gee, S. J.; Hammock, B. D.; Xu, T. *Anal. Chem.* **2019**, *91*, 1532−1540.
(17) Cui, Y.; Li, D.; Morisseau, C.; Dong, J.-X.; Yang, J.; Wan, D.; Rossotti, M.; Gee, S.; González-Sapienza, G.; Hammock, B. *Anal. Bioanal. Chem.* **2015**, *407*, 7275−7283.
(18) Vasylieva, N.; Kitamura, S.; Dong, J.; Barnych, B.; Hvorecny, K. L.; Madden, D. R.; Gee, S. J.; Wolan, D. W.; Morisseau, C.; Hammock, B. D. *Anal. Chim. Acta* **2019**, *1057*, 106−113.
(19) Morisseau, C.; Hammock, B. D. *Annu. Rev. Pharmacol. Toxicol.* **2013**, *53*, 37−58.
(20) Yao, L.; Cao, B.; Cheng, Q.; Cai, W.; Ye, C.; Liang, J.; Liu, W.; Tan, L.; Yan, M.; Li, B.; He, J.; Hwang, S. H.; Zhang, X.; Wang, C.; Ai, D.; Hammock, B. D.; Zhu, Y. *Am. J. Physiol. Gastrointest. Liver Physiol.* **2019**, *316*, G527−G538.
(21) Imig, J. D.; Hammock, B. D. *Nat. Rev. Drug Discovery* **2009**, *8*, 794−805.
(22) Morisseau, C.; Hammock, B. D. *Annu. Rev. Pharmacol. Toxicol.* **2005**, *45*, 311−333.
(23) Lee, K. S. S.; Yang, J.; Niu, J.; Ng, C. J.; Wagner, K. M.; Dong, H.; Kodani, S. D.; Wan, D.; Morisseau, C.; Hammock, B. D. *ACS Cent. Sci.* **2019**, *5*, 1614−1624.
(24) Ren, Q.; Ma, M.; Yang, J.; Nonaka, R.; Yamaguchi, A.; Ishikawa, K.-i.; Kobayashi, K.; Murayama, S.; Hwang, S. H.; Saiki, S.; et al. *Proc. Natl. Acad. Sci. U. S. A.* **2018**, *115*, E5815−E5823.
(25) Borlongan, C. V. *Proc. Natl. Acad. Sci. U. S. A.* **2018**, *115*, 6322−6324.
(26) Yu, Z.; Davis, B. B.; Morisseau, C.; Hammock, B. D.; Olson, J. L.; Kroetz, D. L.; Weiss, R. H. *Am. J. Physiol. Renal Physiol.* **2004**, *286*, F720−F726.
(27) Pérez de la Lastra, J. M.; van den Berg, C. W.; Bullido, R.; Almazan, F.; Dominguez, J.; LLanes, D.; Morgan, B. P. *Immunology* **1999**, *96*, 663−670.
(28) Wilson, M. B.; Nakane, P. K. Recent Development in the Periodate Methods of Conjugating Horseradish Peroxidase (HRPO) to Antibodies. In *Immunofluorescence and Related Staining Techniques*; Elsevier/North Holland Biomedical Press: Amsterdam, 1978; pp 215−224.
(29) Joshi, K. S.; Hoffmann, L. G.; Butler, J. E. *Mol. Immunol.* **1992**, *29*, 971−981.
(30) Butler, J. E.; Ni, L.; Nessler, R.; Joshi, K. S.; Suter, M.; Rosenberg, B.; Chang, J.; Brown, W. R.; Cantarero, L. A. *J. Immunol. Methods* **1992**, *150*, 77−90.
(31) Suter, M.; Butler, J. E. *Immunol. Lett.* **1986**, *13*, 313−316.
(32) Näreoja, T.; Määttänen, A.; Peltonen, J.; Hänninen, P. E.; Härmä, H. *J. Immunol. Methods* **2009**, *347*, 24−30.
(33) Hoffman, W. L.; Jump, A. A. *Anal. Biochem.* **1989**, *181*, 318−320.
(34) Vogt, R. F.; Phillips, D. L.; Henderson, L. O.; Whitfield, W.; Spierto, F. W. *J. Immunol. Methods* **1987**, *101*, 43−50.
(35) MacDougall, D.; Crummett, W. B.; et al. *Anal. Chem.* **1980**, *52*, 2242−2249.
(36) Duhamel, R. C.; Johnson, D. A. *J. Histochem. Cytochem.* **1985**, *33*, 711−714.
(37) Vincent, P.; Samuel, D. *J. Immunol. Methods* **1993**, *165*, 177−182.
(38) Hou, L.; Tang, Y.; Xu, M.; Gao, Z.; Tang, D. *Anal. Chem.* **2014**, *86*, 8352−8358.
(39) Zhu, M.; Gong, X.; Hu, Y.; Ou, W.; Wan, Y. *J. Transl. Med.* **2014**, *12*, 352−361.
(40) Rossotti, M. A.; Pirez, M.; Gonzalez-Techera, A.; Cui, Y.; Bever, C. S.; Lee, K. S. S.; Morisseau, C.; Leizagoyen, C.; Gee, S.; Hammock, B. D.; González-Sapienza, G. *Anal. Chem.* **2015**, *87*, 11907−11914.

https://dx.doi.org/10.1021/acs.analchem.0c01115
Anal. Chem. XXXX, XXX, XXX−XXX